Sensors and Materials, Vol. 38, No. 6 (2026) 3347–3364
MYU Tokyo

S & M 4507

Numerical Performance Assessment of a Rotational Fender System for Ship Impact Mitigation of Marine Structures

Sang-Yeop Lee,[1] Byeongki Ahn,[2] Wonhyeon Kim,[2]
Seungjun Shin,[2] Giryung Kang,[2] and Woo-Dong Lee[2*]

[1]Earthquake Disaster Reduction Center, National Disaster Management Research Institute,
365, Jongga-ro, Jung-gu, Ulsan 44538, Republic of Korea
[2]Department of Ocean Civil Engineering, Gyeongsang National University,
2, Tongyeonghaean-ro, Tongyeong-si, Gyeongsangnam-do 53064, Republic of Korea

(Received December 1, 2025; accepted June 11, 2026)

Keywords: ship collision damage, protective dolphin, dynamic contact analysis, ship–structure impact simulation, impact–rotation energy conversion

Ship–structure collisions pose a significant threat to coastal and offshore infrastructures such as bridge piers, breakwaters, and protective dolphins. In this study, we investigate the performance of a rotational fender system (RFS) that dissipates ship-collision energy through the rolling-induced conversion of translational kinetic energy into rotational kinetic energy. Numerical simulations were conducted using LS-DYNA for ship-collision velocities of 5, 7, and 10 kn and collision angles of 0–75°, with the angles configured to reflect the realistic approach directions of a drifting ship after losing maneuvering control. Within these simulations, the collision response was quantified using a numerical sensing approach. The RFS reduced the peak impact force by 71.47–92.60%, with an average reduction of 83.15%, and delayed the occurrence of the peak force by 0.190–0.464 s. Although the absolute impact force increased with velocity, the reduction efficiency remained consistent, confirming the robustness of the system. These results demonstrate that the RFS effectively transforms impulsive collision loads into gradual and time-distributed responses, alleviating dynamic amplification and local stress concentration. The RFS thus provides a lightweight, modular, and retrofittable protection technology suitable for both new and existing marine infrastructures, which enhances the structural safety and cost-effectiveness of marine infrastructures under realistic drift-collision scenarios.

1. Introduction

The continuous expansion of global maritime transport has led to considerable increases in ship size, cargo capacity, and navigational frequency, which in turn elevates the risk of ship–structure collisions in coastal and offshore regions. According to the United Nations Conference on Trade and Development, the global volume of maritime trade has more than doubled over the past three decades, with an annual growth rate of approximately 2.4% in 2023 compared with

*Corresponding author: e-mail: wdlee@gnu.ac.kr
https://doi.org/10.18494/SAM6184

ISSN 0914-4935

2022.[1] This remarkable growth is closely linked to global economic development, particularly in the container shipping industry, which has experienced a sharp rise in both ship tonnage and operational frequency.

Over the past 15 years, the total number of registered ships worldwide has increased by nearly 53% and the combined gross tonnage by approximately 47%.[2] The European Maritime Safety Agency reported that between 2014 and 2021, a total of 21,173 maritime accidents were recorded, averaging 2647 incidents annually.[3] As maritime traffic density continues to increase, the probability of large-scale collisions involving ultra large container ships (ULCSs) and critical infrastructures, such as bridges, offshore platforms, and harbor facilities, has also grown.

Ship–structure collisions are typically attributed to a combination of human, mechanical, and environmental factors.[4] Human errors, such as operational negligence or navigation misjudgment, account for nearly 80–85% of marine accidents. Mechanical failures, including propulsion loss and steering malfunction, have also contributed to several catastrophic events. For instance, the 2024 Francis Scott Key Bridge collapse in Baltimore occurred when the containership Dali lost power and steering control, leading to a direct collision with the bridge pier.[5] Environmental factors, such as strong currents, high winds, and poor visibility, can further exacerbate collision risks, as illustrated by the 2018 Sky Gate Bridge incident in Japan, where a tanker drifted off its moorings during Typhoon Jebi (T1821) and struck the bridge. In Korea, similar accidents have occurred in port and bridge areas. The 2019 Sea Grand incident at Gwangan (Diamond) Bridge resulted in significant structural damage due to a drunk captain's operational error.[6] These events highlight the critical vulnerability of major coastal infrastructures, such as bridges, breakwaters, and harbor facilities, when subjected to impacts from large ships or drifting objects. Collectively, these cases indicate that ship–structure collisions can occur under diverse operational and environmental conditions, resulting in impact scenarios with substantially different directions, intensities, and energy-transfer characteristics.

In this context, conventional protective dolphin systems and fenders are typically constructed from reinforced concrete or rubber materials and are designed mainly to resist static or quasi-static loads. However, as ship sizes and kinetic energies increase, these traditional systems exhibit inherent limitations. The energy dissipation mechanism of conventional fenders relies mainly on the localized deformation or crushing of materials, which becomes insufficient when dealing with ships exceeding 10000 tons. For example, the protective dolphin system at the Incheon Bridge, a representative large-scale installation, has a diameter of approximately 50 m and a mass of about 1350 t. Although structurally robust, such massive installations demand high construction and maintenance costs and pose logistical challenges during underwater placement.

Studies aimed at improving protection systems against ship collisions have introduced devices designed to absorb collision energy and fender materials with enhanced mechanical performance. Crashworthy devices have been proposed to mitigate ship–bridge collisions by reducing impact force and energy transfer during collision.[7] Steel and ultra high-performance fiber-reinforced concrete composite fenders have also been investigated for bridge protection under vessel collision through experiments and numerical simulations, demonstrating their potential to improve impact resistance and energy absorption capacity.[8] In addition, numerical

analyses using LS-DYNA have been conducted to evaluate the performance of different fender configurations for offshore wind turbine tripod structures subjected to ship impact, emphasizing the importance of fender material selection and energy absorption mechanisms in marine collision protection.[9] These studies indicate that the performance of marine protection systems depends not only on structural strength but also on the capacity to dissipate or redistribute collision energy during impact.

Moreover, as the magnitude of ship impact energy increases in proportion to the ship's displacement and to the square of the impact velocity, simply enlarging the scale of protective structures is not an economically sustainable solution. The need for an innovative system that can dynamically convert and dissipate impact energy rather than relying on material deformation has become increasingly evident.

Therefore, a novel type of marine collision protection system must be developed to improve structural safety and cost efficiency simultaneously. Such a system should effectively reduce impact forces, transform kinetic energy into a secondary form (such as rotation), and mitigate localized stress concentrations on structural members through energy conversion and dissipation mechanisms. For this performance assessment, the relevant impact responses were quantified in LS-DYNA using a numerical sensing approach.

2. Research Concept and Objectives

To address these limitations, in this study, we propose a new concept of a rotational fender system (RFS) designed to dissipate ship impact energy through a rolling mechanism. The RFS converts the linear kinetic energy generated during a ship–structure collision into rotational kinetic energy, thereby reducing the transmitted impact forces. This approach was inspired by the rolling-barrier guardrail used in roadway safety systems, which has demonstrated exceptional performance in absorbing vehicular collision energy by converting it into roller motion.[10]

By applying this principle to marine environments, the proposed system aims to enhance both structural resilience and economic feasibility. When a ship collides with the rotational fender, part of its momentum is absorbed and transferred into rotational motion, reducing the impact energy transmitted to the protective structure. This dynamic energy conversion and dissipation mechanism offers a practical advantage over conventional static systems, allowing for a lighter, more adaptable design capable of withstanding high-energy impacts.

The numerical simulation was conducted using LS-DYNA,[11] which enables the accurate computation of dynamic contact interactions between the ship, the rotational fender, and the protective structure (dolphin). Using LS-DYNA, we performed detailed numerical modeling of ship-collision scenarios, including variations in ship-collision angle and velocity. The arbitrary Lagrangian–Eulerian (ALE) method is employed to represent the nonlinear interaction between fluids and structures while maintaining numerical stability.[12]

The main objectives of this study are summarized as follows:

- to verify the reliability of LS-DYNA for ship–structure (in particular, ship–dolphin) collision analysis through comparison with existing experimental data,[13]

- to elucidate the energy conversion mechanism from translational to rotational motion and the dissipation mechanism of the RFS during ship-collision impacts,
- to evaluate reductions in the peak impact forces achieved by the RFS under various ship-collision angles and velocities, and
- to discuss the structural and economic implications of applying the RFS as a protective measure for major coastal and offshore infrastructures.

Ultimately, the findings of this study contribute to the design of next-generation marine protective systems that achieve both structural efficiency and high safety performance against ship collisions.

3. Numerical Methodology

To numerically analyze the dynamic response of ship–structure collisions involving the proposed RFS, the commercial finite element software LS-DYNA was employed. LS-DYNA is well known for its capability to handle highly nonlinear, transient problems such as impact, explosion, and fluid–structure interaction (FSI) through explicit time integration. LS-DYNA's explicit time integration method was used to simulate the nonlinear dynamic behavior during ship–structure collisions.

3.1 LS-DYNA

The ALE formulation introduces an intermediate reference frame between the Lagrangian and Eulerian descriptions, enabling the mesh to move independently of the material. This characteristic is particularly advantageous for FSI simulations, where the interaction of fluid and solid boundaries requires both accuracy and numerical stability. The general ALE transport equation can be written as

$$\frac{\partial f\left(X_i,t\right)}{\partial t}=\frac{\partial f\left(x_i,t\right)}{\partial t}-w_i\frac{\partial f\left(x_i,t\right)}{\partial x_i}, \tag{1}$$

where X_i represents the Lagrangian (material) coordinates and x_i the Eulerian (spatial) coordinates. The material velocity is represented by v_i and the mesh velocity by u_i, such that the relative mesh velocity is defined as $w_i = v_i - u_i$.

The conservation laws of mass, momentum, and energy in the ALE framework are expressed as

$$\frac{\partial \rho}{\partial t}=-\rho\frac{\partial v}{\partial x_i}-w_i\frac{\partial \rho}{\partial x_i}, \tag{2}$$

$$\rho\frac{\partial v}{\partial t}=-\left(\sigma_{ij,j}+\rho b_i\right)-\rho w_i\frac{\partial v_i}{\partial x_j}, \tag{3}$$

$$\frac{\partial E}{\partial t} = -\left(\sigma_{ij} v_{i,j} + \rho b_i v_j\right) - \rho w_j \frac{\partial E}{\partial x_j}, \tag{4}$$

where ρ represents the density, σ_{ij} the stress tensor, b_i the body acceleration (e.g., gravity), and E the internal energy.

The Courant–Friedrichs–Lewy (CFL) condition was imposed to ensure numerical stability during the explicit time integration process. This criterion limits the time increment so that numerical information does not propagate across more than one element per step, maintaining both stability and accuracy in simulating high-speed impact phenomena such as ship–structure collisions.

3.2 Model validation

To verify the reliability of LS-DYNA for ship–structure collision analysis, a validation study was performed using experimental data from a previous study on the collision of a drifting container with a vertical column under solitary wave conditions.[13] The numerical domain was constructed on the basis of this experiment, divided into the wave field analysis region and the collision analysis region (Fig. 1). The wave field was simulated using a numerical wave tank,[14] and the free surface elevation and velocity fields during wave overtopping were applied as incident conditions on the ocean side of the LS-DYNA collision simulation.

The results of the top-view comparison of the container's drift trajectory were obtained from a camera mounted above the wave flume and compared with the LS-DYNA simulation results (Fig. 2). The agreement between the experimental and simulated trajectories confirmed the model's capability in capturing the container's drift behavior.

For quantitative validation, Fig. 3 shows the results of the comparison of the container's drift velocity distribution derived from the experimental video analysis and the impact force on the column measured by load cells, compared with the LS-DYNA results. The simulation accurately predicted both the velocity distribution and the impact force, validating the model's performance.

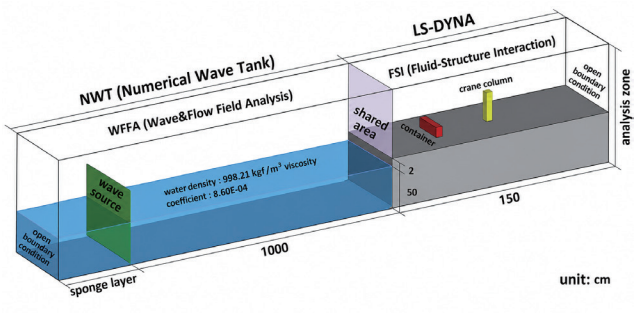

Fig. 1. (Color online) Numerical domain constructed on the basis of Hwang *et al.*'s[13] experiment showing both wave and collision analysis regions.

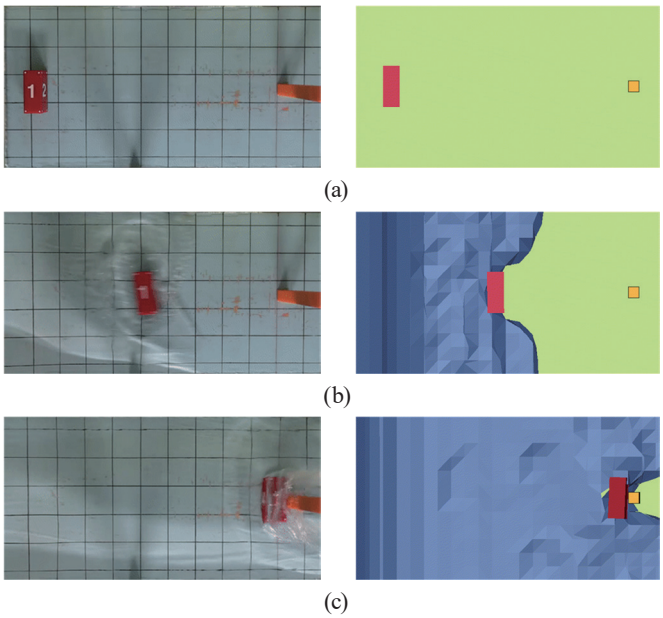

Fig. 2. (Color online) Results of comparison between experimental observations (left) and LS-DYNA simulations (right) of container drift and impact behavior. (a) $t = 0$ s, (b) $t = 0.65$ s, and (c) $t = 0.92$ s.

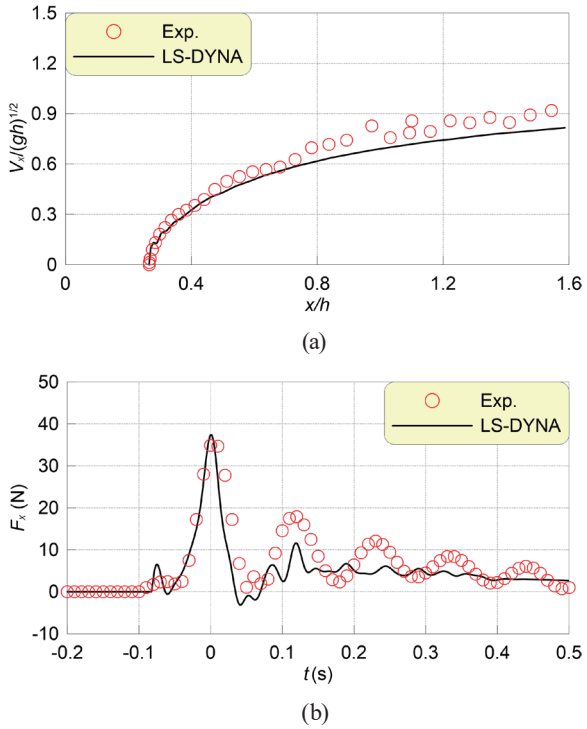

Fig. 3. (Color online) Results of comparison of (a) container drift velocity distribution and (b) impact force acting on a vertical structure.

These validation results demonstrate the validity and effectiveness of LS-DYNA in simulating the collision process, and thus, it is utilized in this study for the numerical collision analysis of the proposed RFS.

3.3 Numerical modeling

The geometric and material configurations were determined on the basis of real-scale engineering data and design standards. The numerical model comprises three main components:

- Protective structure: The base structure was modeled after the protective dolphin installed at the Incheon Bridge [Fig. 4(a)]. The structure was assumed to be cylindrical with a diameter of 25 m and a height of 50 m. It was made of normal-strength concrete with a compressive strength of 40 MPa, a tensile strength of 4 MPa, an elastic modulus of 31 GPa, and a density of 2,400 kg/m^3. The base of the protective dolphin was fixed to simulate the pile foundation anchorage condition.
- Fender system: The proposed RFS was modeled as a steel cylindrical ring with an inner diameter of 25 m, an outer diameter of 30 m, and a thickness of 2.5 m [Fig. 4(b)]. The material properties correspond to structural carbon steel with a density of 7850 kg/m^3, an elastic modulus of 200 GPa, and a Poisson's ratio of 0.3. The RFS was positioned concentrically around the protective dolphin, allowing free rotational motion about the central axis upon collision, thereby enabling energy conversion and dissipation through rolling.
- Ship model: The ship hull geometry was adapted from the Korea Research Institute of Ships & Ocean Engineering's container ship (KCS) model,[15] scaled up to represent a 24000 TEU container ship with a length of 400 m, a beam of 61 m, and a height of 33 m [Fig. 4(c)]. The ship's material was modeled as a rigid body, emphasizing the transfer of ship-collision energy and the structural response of the RFS and protective dolphin, rather than hull deformation.

This rigid-body assumption is commonly adopted in ship-impact studies where the primary interest lies in the response of the target structure rather than the detailed hull deformation, and it provides a conservative estimate of the forces transmitted to the protective structure.

3.4 Simulation setup

The simulation assumes a realistic accident scenario in which a large container ship loses both steering and propulsion control before colliding with a fixed coastal structure. During the Baltimore bridge collapse in 2024, a container ship in a loss-of-control condition struck a bridge pier at an approximate velocity of 6.8 kn (3.50 m/s).[5] In addition, according to the Incheon

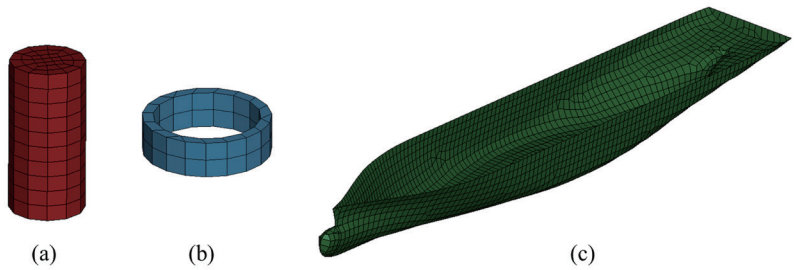

Fig. 4. (Color online) Numerical models: (a) protective dolphin, (b) RFS, and (c) KCS hull.

Regional Office of Oceans and Fisheries, Ministry of Oceans and Fisheries, Republic of Korea,[16] ships exceeding 50000 GT must navigate at speeds below 10 kn (5.14 m/s) when passing through the Incheon Bridge, while those over 160000 tons are limited to 6 kn (3.09 m/s) or less.

Considering these accident records and navigation regulations, representative ship-collision velocities of 5, 7, and 10 kn (2.57, 3.60, and 5.14 m/s, respectively) were selected for numerical simulation. To reproduce realistic drift-collision conditions, the ship-collision angle, defined as the angle between the ship's drift (velocity) direction and its longitudinal axis, was configured by considering the possible approach orientations of a ship under loss of maneuverability. Accordingly, six representative collision angles (0, 15, 30, 45, 60, and 75°) were applied to reflect diverse drift paths and energy levels at impact.

The computational domain was configured to ensure a sufficiently wide interaction region among the ship, RFS, and protective dolphin, allowing the accurate evaluation of impact response (Fig. 5). The AUTOMATIC_GENERAL contact algorithm in LS-DYNA was employed to automatically detect and compute multi body contact behavior during high-speed impacts. In the contact interface between the RFS and the protective dolphin, Coulomb friction was explicitly defined using static and dynamic friction coefficients of 0.30 and 0.20, respectively, to represent realistic tangential resistance at the steel–concrete interface. To maintain numerical stability and satisfy the CFL condition, the initial time step for explicit integration was set to 1.0×10^{-5} s.

The impact force acting on the protective dolphin was obtained from the SPCFORC output in LS-DYNA. SPCFORC records the reaction forces at nodes constrained by single-point constraints (SPCs). In this study, the resultant reaction force at the constrained region of the protective dolphin was adopted as the force transmitted to the target structure, analogous to the reaction force measured by load cells in physical experiments.

4. Numerical Results

4.1 Collision response and energy conversion mechanism

The collision simulations between the ship and the protective dolphin demonstrate that the RFS fundamentally alters how impact energy is transmitted to the structure. Figure 6 presents the time histories of the impact force acting on the protective dolphin and the roller's angular velocity for a ship-collision velocity of 7 kn and a collision angle of 0° (head-on impact), with

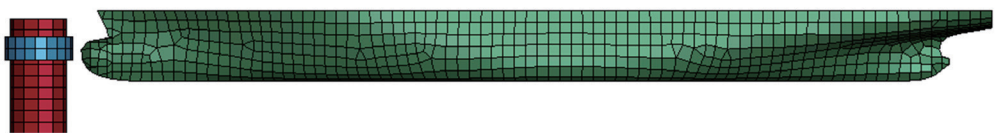

Fig. 5. (Color online) Computational domain showing the interaction region among the ULCS, RFS, and protective dolphin.

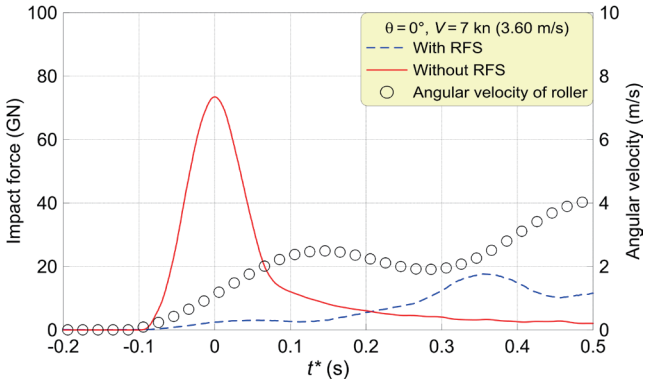

Fig. 6. (Color online) Time histories of the impact force acting on the protective dolphin and the roller's angular velocity, with and without the RFS.

and without the RFS. In the figure, the time axis is expressed as t^*, which represents a time-shifted variable defined by $t^* = t - t_p$, where t_p denotes the time at which the peak impact force occurs without the RFS. This time shift was introduced to analyze the delay in the occurrence of the peak impact force caused by the installation of the RFS.

Without the RFS, the ship's bow directly strikes the fixed protective dolphin, producing a sharp impulsive load of about 73.5 GN within a very short contact period. Because the contact point remains nearly stationary, the impact energy is concentrated over a small area and short duration, leading to severe stress concentration on the protective dolphin surface. When the RFS is installed, the contact changes from a normal indentation to a rolling interaction. The roller begins to rotate at the moment of impact, and a portion of the ship's translational kinetic energy is converted into the rotational kinetic energy of the fender. This conversion reduces the effective normal deceleration of the ship and thereby decreases the peak impact force transmitted to the protective dolphin. As a result, the peak force drops to 17.6 GN (76.01% reduction), and its occurrence is delayed by about 0.355 s.

The roller's rotational inertia acts as a dynamic energy buffer, as the work required to accelerate the roller is extracted directly from the ship's translational kinetic energy. Consequently, the impact-force response evolves more gradually, exhibiting a smooth rise and decay rather than an abrupt peak, which alleviates localized deformation demands on the protective dolphin surface. This rotational mechanism fundamentally modifies the energy transfer process, transforming the collision from a short-duration impulsive event into a time-distributed interaction. The extended duration of force transmission implies that the same collision energy is delivered over a longer time interval, effectively reducing the rate of momentum exchange and the associated dynamic amplification of structural response.

4.2 Effect of ship-collision angle

The effect of ship-collision angle was investigated for six approach angles, and the results were presented for a representative ship-collision velocity of 7 kn. Figure 7 presents the time histories of the impact force acting on the protective dolphin and the roller's angular velocity at a

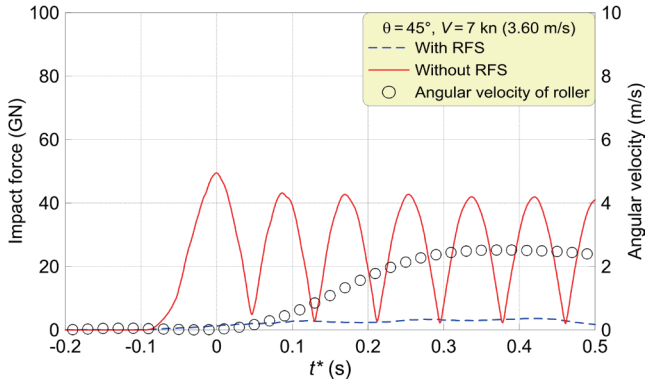

Fig. 7. (Color online) Time histories of the impact force acting on the protective dolphin and the roller's angular velocity at a ship-collision angle of 45°, with and without the RFS.

collision angle of 45°, with and without the RFS, whereas Fig. 8 shows the impact-force time histories for all collision angles under the same conditions. The corresponding reductions in peak impact force and delay time are summarized in Table 1.

As shown in Fig. 7, when the ship collides at an oblique angle such as 45°, the impact force transmitted to the protective dolphin becomes much smaller than that in the head-on collision (Fig. 6), because the bow's tangential motion allows a portion of the kinetic energy to be redirected along the contact surface rather than being fully transferred in the normal direction. The case without the RFS exhibits a distinct oscillatory pattern in the impact-force time history, which is not observed in the head-on collision. This oscillation results from the repeated contact–release behavior between the ship's bow and the protective dolphin surface during oblique impact, where the contact point continuously shifts along the curved interface. Each intermittent contact and separation generates localized peaks and troughs in impact force, producing a periodic fluctuation.

In contrast, when the RFS is installed, this oscillatory behavior is almost completely suppressed because the roller absorbs tangential motion through continuous rotation, thereby smoothing the force transmission. Under the 45° condition, the RFS further enhances this effect by converting the tangential component of the ship's kinetic energy into the roller's rotational motion. As a result, the peak impact force acting on the protective dolphin decreases from 49.47 GN (without RFS) to 3.66 GN (with RFS), corresponding to a 92.6% reduction. The roller exhibits a gradual and continuous increase in angular velocity, indicating that the energy is dissipated progressively through rolling rather than instantaneously through compression. Therefore, oblique collisions provide a more favorable condition for the RFS to transform impact energy into rotational kinetic energy, leading to a smoother and more efficient energy dissipation process.

The results in Fig. 8 support these observations by showing the variation of impact-force time histories for all collision angles. As the collision angle increases from 0 to 75°, the peak impact force without the RFS decreases from 73.45 to 20.00 GN, whereas with the RFS, it decreases from 17.62 to 2.06 GN. The corresponding reduction ratios range from 76.0% (0°) to 89.7% (75°), with an average reduction of 83.2% across all cases (Table 1). The peak-force occurrence is

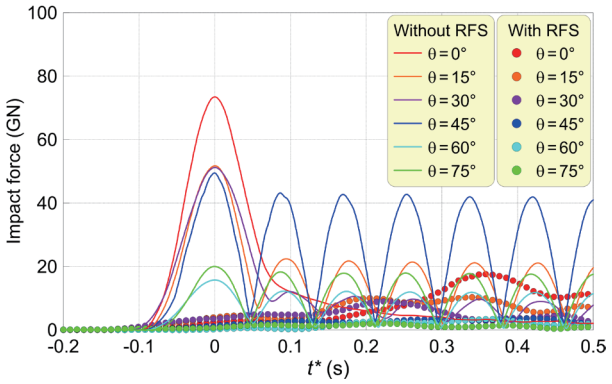

Fig. 8. (Color online) Results of comparison of the impact forces acting on the protective dolphin at various ship-collision angles, with and without the RFS.

Table 1
Peak impact force, reduction ratio, and delay time according to ship-collision angle at a velocity of 7 kn.

Collision angle (°)	Peak impact force (GN)		Reduction ratio (%)	Delay time (s)
	Without RFS	With RFS		
0	73.45	17.62	76.01	0.355
15	51.72	10.33	80.03	0.341
30	51.21	9.04	82.35	0.227
45	49.47	3.66	92.60	0.414
60	15.74	3.38	78.53	0.359
75	20.00	2.06	89.70	0.221
Average	43.60	7.68	83.20	0.320

delayed by 0.221–0.414 s, with an average delay time of 0.320 s, confirming that the RFS extends the impact duration and mitigates impulsive loading on the protective dolphin through rolling-induced energy redistribution.

Together, the results suggest that oblique impacts not only generate inherently smaller forces but also enable the RFS to perform more effectively by facilitating rotational energy conversion and time-dependent energy dissipation.

4.3 Effect of ship-collision velocity

The effect of ship-collision velocity was examined for three representative speeds of 5, 7, and 10 kn, and the results were presented for a fixed ship-collision angle of 45°. Figure 9 shows the time histories of the impact force acting on the protective dolphin and the roller's angular velocity at a collision velocity of 10 kn, with and without the RFS, while Fig. 10 shows the variation of impact-force time histories for all collision velocities under the same impact angle. The corresponding reductions in peak impact force and delay time are summarized in Table 2.

When the ship collides at 10 kn (Fig. 9), a larger collision energy is generated compared with the 7 kn case (Fig. 7), resulting in a stronger impulsive response in the absence of the RFS. The peak impact force without the RFS reaches 59.26 GN, whereas with the RFS, it is reduced to 6.84 GN, corresponding to a reduction ratio of 88.5%. Despite the higher initial kinetic energy,

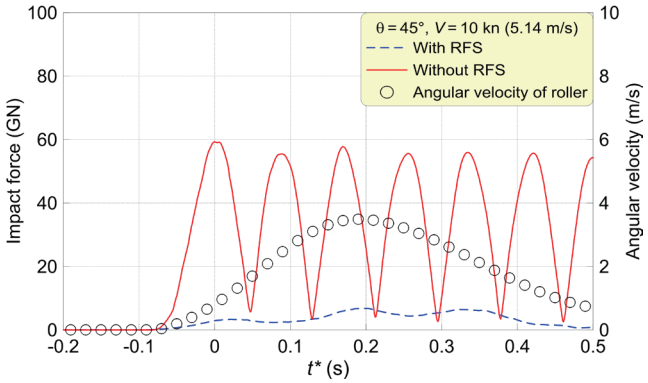

Fig. 9. (Color online) Time histories of the impact force acting on the protective dolphin and the roller's angular velocity at a ship-collision velocity of 10 kn, with and without the RFS.

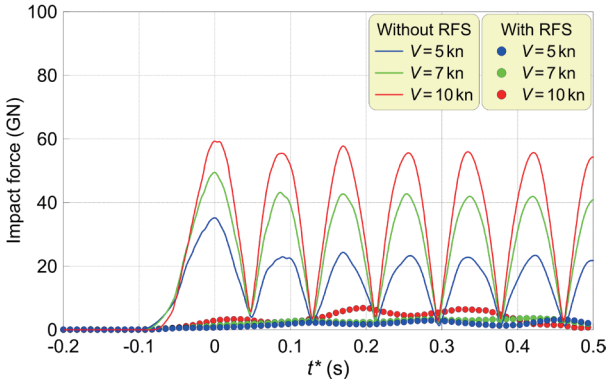

Fig. 10. (Color online) Results of comparison of the impact forces acting on the protective dolphin at various ship-collision velocities, with and without the RFS.

Table 2
Peak impact force, reduction ratio, and delay time according to ship-collision velocity at a collision angle of 45°.

Collision velocity (kn)	Peak impact force (GN)		Reduction ratio (%)	Delay time (s)
	Without RFS	With RFS		
5	35.20	3.22	90.85	0.458
7	49.47	3.66	92.60	0.414
10	59.26	6.84	88.46	0.194
Average	47.98	4.57	90.64	0.355

the roller exhibits a faster and more pronounced rotational acceleration, demonstrating that a substantial portion of the impact energy is converted into rotational motion. This conversion mitigates the impulsive loading on the protective dolphin by distributing the contact force over time, thereby reducing both the magnitude and sharpness of the impact response.

Figure 10 illustrates the general trend that as the collision velocity increases, the impact force acting on the protective dolphin also increases in both cases, with and without the RFS, owing to the quadratic dependence of kinetic energy on velocity. However, the rate of increase in impact force is significantly lower when the RFS is installed. This finding shows that the rotational

kinetic energy–dissipation mechanism effectively limits the transmission of high-magnitude impact loads.

According to Table 2, the RFS reduces the peak impact force by 90.9% at 5 kn, 92.6% at 7 kn, and 88.5% at 10 kn, with an average reduction ratio of 90.6% across all velocities. The occurrence of peak impact force is delayed by 0.194–0.458 s, with an average delay of 0.355 s, confirming that the RFS consistently extends the impact duration and smooths the force transmission over a wider time interval.

Overall, the results show that although collision energy increases rapidly with ship velocity, the RFS maintains high impact-attenuation performance even under severe conditions. This stability arises from the roller's ability to absorb and dissipate excess kinetic energy through rotational motion, preventing excessive stress concentration on the protective dolphin.

5. Discussion

5.1 Impact mitigation performance of the RFS

The overall performance of the RFS was evaluated under three representative ship-collision velocities of 5, 7, and 10 kn. To reproduce realistic drift-collision conditions, the collision angles were defined by considering the possible approach orientations of a ship that has lost steering and propulsion control. The representative results at 7 kn, previously presented in Table 1, serve as a reference for comparison, while Tables 3 and 4 show the peak impact forces and delay times with and without the RFS for the 5 and 10 kn cases, respectively.

Table 3
Peak impact force, reduction ratio, and delay time according to ship-collision angle at a velocity of 5 kn.

Collision angle (°)	Peak impact force (GN)		Reduction ratio (%)	Delay time (s)
	Without RFS	With RFS		
0	53.16	10.97	79.36	1.046
15	36.84	6.34	82.79	0.388
30	31.60	4.38	86.14	0.295
45	35.20	3.22	90.85	0.458
60	11.24	2.27	79.80	0.396
75	14.29	1.54	89.22	0.200
Average	30.39	4.79	84.70	0.464

Table 4
Peak impact force, reduction ratio, and delay time according to ship-collision angle at a velocity of 10 kn.

Collision angle (°)	Peak impact force (GN)		Reduction ratio (%)	Delay time (s)
	Without RFS	With RFS		
0	106.41	27.43	74.22	0.235
15	74.10	21.14	71.47	0.229
30	78.40	13.61	82.64	0.275
45	59.26	6.84	88.46	0.194
60	22.50	4.50	80.00	0.154
75	28.54	2.13	92.54	0.051
Average	61.54	12.61	81.55	0.190

The results reveal a consistent trend across all cases. At every velocity, the RFS substantially reduces the peak impact force transmitted to the protective dolphin. For the 7 kn case (Table 1), the average reduction ratio is 83.20%, whereas for the 5 and 10 kn cases (Tables 3 and 4, respectively), the average reductions are 84.70 and 81.55%, respectively. This indicates that the RFS maintains a high mitigation efficiency, generally above 80%, regardless of impact energy. Although the absolute impact force increases with velocity owing to the quadratic dependence of kinetic energy on speed, the relative attenuation capability of the RFS remains nearly constant, demonstrating that the system scales effectively under higher collision intensities.

Another notable feature is the reduction in the delay time of the peak impact force with increasing velocity. The average delay time decreases from 0.464 s at 5 kn to 0.320 s at 7 kn and 0.190 s at 10 kn. This shortening reflects the more rapid energy transfer that occurs as kinetic energy increases. Nevertheless, the persistence of a measurable delay at all speeds indicates that the RFS still redistributes the collision load over time. The temporal spreading of the impact force, produced by the roller's rotational inertia, plays a crucial structural role: it reduces dynamic amplification, alleviates stress concentration on the protective dolphin surface, and promotes a quasi-static load-transfer behavior. Consequently, the RFS transforms an impulsive collision into a controlled, time-distributed energy-dissipation process, thereby improving structural stability and reducing damage potential.

Overall, these findings confirm that the RFS provides robust and scalable impact mitigation across various collision velocities. Even as impact energy increases under uncontrolled drift conditions, the system retains its capability to attenuate peak force and extend impact duration, offering a practical and reliable protection measure for coastal and offshore infrastructures.

5.2 Structural and economic considerations

The application of the RFS as a protective measure for major coastal and offshore infrastructures provides both structural and economic benefits. Structurally, the RFS alleviates the instantaneous concentration of impact loads acting on protective dolphins, bridge piers, and offshore wind turbine foundations, thereby reducing the likelihood of local damage. This enables the design of more durable and resilient structures with optimized safety factors.

Because the collision energy is dissipated dynamically through rotational motion rather than static deformation, the required material volume can be significantly reduced compared with that in the case of conventional massive concrete dolphins. Furthermore, the lightweight and modular design of the RFS facilitates easier installation and maintenance. The RFS can also be retrofitted to existing port and bridge facilities without major reconstruction, thereby enhancing the overall cost efficiency of coastal and offshore infrastructures.

Taken together, these findings indicate that the RFS can serve as an efficient and sustainable protective system capable of absorbing ship-collision energy and minimizing transmitted impact forces. From an economic standpoint, the reduced material demand and modular installation of the RFS can lower construction and maintenance costs compared with those of conventional massive concrete dolphins, particularly for retrofitting existing bridges and harbor facilities.

5.3 Limitations and future work

Although this study successfully demonstrated the impact-mitigation performance of the RFS through numerical simulations, several limitations remain to be addressed for practical application.

- The attachment method between the RFS and the protective dolphin has not yet been investigated. Further research is required to develop joint mechanisms capable of maintaining rotational freedom while reliably transmitting tangential forces under impact loading. Comprehensive field-scale testing under various hydrodynamic conditions is recommended.
- The RFS must be capable of responding adaptively to hydrodynamic variations such as tidal fluctuations and wave-induced water-level changes. Designing the RFS with appropriate buoyancy characteristics can allow it to maintain optimal performance under dynamically changing sea levels.
- The selection of suitable materials for the RFS remains a critical issue. Materials with high corrosion resistance, fatigue strength, and low specific weight, such as stainless steel, aluminum alloys, or fiber-reinforced composites, should be experimentally validated to ensure long-term durability in marine environments.
- The reduction in friction between the RFS and the protective dolphin is essential to achieve efficient rotational motion. The application of lubrication systems, polymer liners, or wear-resistant bearing materials should be considered to minimize frictional losses and extend service life.

These issues should be further examined through detailed structural design, experimental verification, FSI simulations, and field testing to enhance the reliability and applicability of the RFS in real marine environments. In addition, recent studies have shown that floating offshore wind turbines are highly vulnerable to ship impacts, particularly under scenarios involving large tankers or drifting ships.[17,18] This suggests that the impact-mitigation concept embodied by the RFS may also be applicable to offshore renewable infrastructures, where hydrodynamic loading and impact risks coexist.

6. Conclusions

In this study, we conducted numerical simulations to evaluate the performance of an RFS in mitigating ship-collision impacts on marine protective structures. Using the LS-DYNA-based ALE framework, we simulated ship–structure collision scenarios for various collision angles (0–75°) and velocities (5–10 kn). To realistically represent drift-collision events, the collision angles were established considering the approach orientations of a ship under loss of steering and propulsion control. Within this framework, the collision response was quantified using a numerical sensing approach to evaluate the impact response transmitted to the protective structure. The results demonstrated that the RFS effectively reduced the peak impact force acting on the protective dolphin by 71.47–92.60%, with an average reduction of 83.15% across all analyzed conditions. At a representative velocity of 7 kn, the RFS achieved the highest mitigation ratio of 92.60% at a collision angle of 45° while maintaining stable attenuation

performance under both low- and high-energy impacts. Although the absolute impact force increases with collision velocity, the reduction efficiency of the RFS remains nearly constant, confirming its applicability to high-energy collision scenarios.

The introduction of rotational motion alters the energy-transfer mechanism between the ship and the structure. The roller's inertia converts part of the translational kinetic energy into rotational kinetic energy, delaying the occurrence of the peak impact force, with the average delay ranging from 0.190 to 0.464 s depending on collision velocity and angle, and transforming the impulsive load into a time-distributed response. This temporal spreading alleviates stress concentration and reduces dynamic amplification on the protective dolphin surface.

From a practical perspective, the RFS provides both structural and economic advantages. The rolling-based dissipation mechanism reduces material demand compared with that in the case of conventional large concrete dolphins, while its lightweight, modular configuration enables easy installation, maintenance, and retrofitting for existing port and bridge facilities.

Overall, the RFS represents a scalable and efficient protection technology capable of effectively dissipating ship-collision energy, reducing local structural damage, and improving the safety and durability of coastal and offshore infrastructures including bridges, dolphins, and offshore wind turbines. By building on this numerical approach, future research will extend the analysis to evaluate impact interactions between waterborne debris—ranging from driftwood transported during river flooding[19,20] to large objects mobilized by tsunamis or storm surges[21,22]—and coastal or hydraulic structures.

Acknowledgments

This work was supported by the National Research Foundation of Korea (NRF) grant funded by the Korea government (MSIT) (RS-2024-00356327).

References

1 United Nations Conf. Trade and Development: Review of Maritime Transport 2024 (United Nations, Geneva, 2024). https://unctad.org/publication/review-maritime-transport-2024 (accessed January 2025).
2 M. Marino, L. Cavallaro, and E. Castro: Data Brief **49** (2023) 109340. https://doi.org/10.1016/j.dib.2023.109340
3 G. Briguglio and V. Crupi: J. Mar. Sci. Eng. **12** (2024) 353. https://doi.org/10.3390/jmse12020353
4 S. Liao, J. Weng, Z. Zhang, Z. Li, and F. Li: J. Mar. Sci. Eng. **11** (2023) 1513. https://doi.org/10.3390/jmse11081513
5 National Transportation Safety Board: Contact of Containership Dali with the Francis Scott Key Bridge and Subsequent Bridge Collapse: Marine Investigation Preliminary Report (DCA24MM031) (National Transportation Safety Board, Washington, DC, 2024). https://www.ntsb.gov/ (accessed January 2025).
6 The Independent: Russian Cargo Ship with "Drunk" Captain on Board Crashes into Motorway Bridge, Tearing Huge Hole (2019). https://www.independent.co.uk/news/world/asia/russia-ship-crash-cargo-drunk-captain-south-korea-a8801766.html (accessed January 2025).
7 L. Wang, L. Yang, D. Huang, Z. Zhang, and G. Chen: Int. J. Impact Eng. **35** (2008) 895. https://doi.org/10.1016/j.ijimpeng.2007.12.005
8 W. Fan, W. Guo, Y. Sun, B. Chen, and X. Shao: Ocean Eng. **165** (2018) 1. https://doi.org/10.1016/j.oceaneng.2018.07.028
9 Z. Han, C. Li, Y. Deng, and J. Liu: Ocean Eng. **194** (2019) 106614. https://doi.org/10.1016/j.oceaneng.2019.106614
10 M. Malewar: New Korean Rolling Barrier System Could Save Millions of Lives, Tech Explorist (2016). https://www.techexplorist.com/new-korean-rolling-guardrail-system-save-millions-lives/4127/ (accessed February 2025).

11 ANSYS, Inc.: LS-DYNA Theory Manual, Version R14 (ANSYS, Inc., Canonsburg, PA, 2025). https://ftp.lstc.com/anonymous/outgoing/web/ls-dyna_manuals/DRAFT/DRAFT_Theory.pdf (accessed January 2026).
12 M. Souli, A. Ouahsine, and L. Lewin: Comput. Methods Appl. Mech. Eng. **190** (2000) 659. https://doi.org/10.1016/S0045-7825(99)00410-4
13 T. G. Hwang, T. Y. Kim, J. W. Kim, Y. J. Kim, and W. D. Lee: J. Earthquake Tsunami **18** (2024) 2450010. https://doi.org/10.1142/S1793431124500106
14 W. D. Lee, G. S. Yeom, J. Kim, S. Lee, and T. Kim: Ocean Eng. **259** (2022) 111897. https://doi.org/10.1016/j.oceaneng.2022.111897
15 Korea Research Institute of Ships and Ocean Engineering: KRISO Standard Ships Data. https://kriso.re.kr/menu.es?mid=a20206000000 (accessed May 2023).
16 Incheon Regional Office of Oceans and Fisheries: Incheon Port and Gyeongin Port Vessel Navigation Regulations, Public Notice No. 2024-133 (Ministry of Oceans and Fisheries, Republic of Korea, 2024). https://www.law.go.kr/LSW/admRulLsInfoP.do?admRulId=2083626&efYd=0 (accessed February 2025).
17 D. H. Yoon and J. Choung: J. Ocean Eng. Technol. **37** (2023) 111. https://doi.org/10.26748/KSOE.2023.004
18 Y. J. Yu, S. H. Park, and S. R. Cho: J. Ocean Eng. Technol. **38** (2024) 124. https://doi.org/10.26748/KSOE.2023.036
19 P. N. De Cicco, E. Paris, L. Solari, and V. Ruiz-Villanueva: J. Flood Risk Manag. **13** (2020) e12599. https://doi.org/10.1111/jfr3.12599
20 T. Okamoto, T. Someya, and M. Sanjou: Proc. River Flow 2020 (CRC Press, 2020) 1630–1638. https://doi.org/10.1201/b22619-229
21 T. Kim, T. Hwang, S. Baek, S. Hong, J. Kim, and W. D. Lee: J. Earthquake Tsunami **17** (2023) 2350016. https://doi.org/10.1142/S1793431123500161
22 W. D. Lee, T. Kim, J. Kim, S. K. Kim, H. Oh, and T. Hwang: J. Ocean Eng. Technol. **38** (2024) 282. https://doi.org/10.26748/KSOE.2024.070

About the Authors

Sang-Yeop Lee received his Ph.D. degree in hydraulic engineering from Gyeongsang National University, Republic of Korea, in 2023. Since 2019, he has been serving as a senior researcher at the Earthquake Disaster Reduction Center in the National Disaster Management Research Institute. His work focuses on coastal hazard impact assessment using numerical modeling for storm surges, tsunamis, and swell waves. (lsy1345@korea.kr)

Byeongki Ahn is an undergraduate student in the Department of Ocean Civil Engineering at Gyeongsang National University, Republic of Korea. He is a student researcher at the Coastal & Ocean Hydro-Morphodynamics Laboratory, where he participates in R&D projects related to coastal disaster prevention. His research interests include FSI analysis and impact assessment of drifting objects. (abk51555@gnu.ac.kr)

Wonhyeon Kim is an undergraduate student in the Department of Ocean Civil Engineering at Gyeongsang National University, Republic of Korea. He is a student researcher at the Coastal & Ocean Hydro-Morphodynamics Laboratory, where he participates in R&D projects related to coastal disaster prevention. His research interests include hydraulic experiments and numerical wave tank analysis. (kwh6273@gnu.ac.kr)

Seungjun Shin received his B.S. degree in ocean civil engineering from Gyeongsang National University, Republic of Korea, in 2025. He is currently studying for his master's degree in hydraulic engineering in the Department of Ocean Civil Engineering at Gyeongsang National University. His research interests include wave–current interaction analysis, the stability evaluation of permeable coastal structures, hydraulic experiments, and numerical wave tank simulation. (2025210194@gnu.ac.kr)

Giryung Kang received his B.S. degree in ocean civil engineering from Gyeongsang National University, Republic of Korea, in 2025. He is currently studying for his master's degree in hydraulic engineering in the Department of Ocean Civil Engineering at Gyeongsang National University. His research interests include sediment erosion and local scour, computational fluid dynamics (CFD), hydraulic model experiments, and fluid–soil interaction analysis. (2025210192@gnu.ac.kr)

Woo-Dong Lee received his Ph.D. degree in coastal and ocean engineering from Nagoya University, Japan, in 2012. From 2012 to 2017, he worked as a research fellow at the Institute of Marine Industry, Gyeongsang National University, Republic of Korea. Since 2017, he has been a professor in the Department of Ocean Civil Engineering at Gyeongsang National University. His research interests include numerical modeling, hydraulic experiments, coastal hazard assessment, marine disasters, and diving engineering. (wdlee@gnu.ac.kr)